Histol Histopathol (2010) 25: 21-32

http://www.hh.um.es

Histology and Histopathology

Cellular and Molecular Biology

Morphological and biochemical patterns in skeletal muscle apoptosis

A. D'Emilio[1], L. Biagiotti[1], S. Burattini[1], M. Battistelli[2], B. Canonico[1,3], C. Evangelisti[4], P. Ferri[1], S. Papa[1,3], A.M. Martelli[4,5] and E. Falcieri[1,5]

[1]DISUAN and [3]Center of Cytometry and Cytomorphology, University of Urbino "Carlo Bo", [2]Laboratory of Cell Biology and Electron Microscopy and [5]IGM, CNR, Rizzoli Orthopaedical Institute, Bologna and [4]Department of Anatomical Sciences, University of Bologna, Italy

Summary. Some neuromuscular disorders, such as Duchenne muscular dystrophy, hereditary inclusion body myopathy, malignant hyperthermia, alcoholic myopathy and mitochondrial myopathies are characterized by oxidative stress and loss of muscle fibres due to apoptosis. In this study we have analyzed muscle cell death *in vitro* utilizing C2C12 myoblasts and myotubes, inducing apoptosis by means of UVB irradiation. C2C12 cells were analysed by scanning and transmission electron microscopy (SEM, TEM) as well as by TUNEL reaction. DNA analysis was performed by gel electrophoresis and flow cytometry. MitoTracker red CMXRos and JC-1 fluorescent probes were also used to study mitochondrial behavior. Finally, caspase activity was investigated by means of Western blot, while caspase-9 and -3 inhibitor effects by means of SEM.

SEM showed the typical membrane blebbing while TEM revealed the characteristic chromatin condensation. The TUNEL reaction presented a certain positivity too. Apoptotic and non-apoptotic nuclei in the same myotube were identified both by TUNEL and TEM.

Gel electrophoresis never showed oligonucleosomal DNA fragmentation, in agreement with the cell cycle analysis performed by flow cytometry which did not reveal a sharp subdiploid peak. Mitochondrial response to UVB was later investigated and a decrease in mitochondrial functionality appeared. Caspase-9 and -3 cleavage, and, consequently, the activation of the caspase cascade, was also demonstrated by Western blot. Moreover a decrease in apoptotic cell number was noted after caspase-9 and-3 inhibitor treatment.

All these results indicated that UVB irradiation induces apoptosis, both in myoblasts and in myotubes, the second being more resistant. DNA fragmentation, at least the nucleosomic type, does not occur. A certain double-strand cleavage appears in TUNEL analysis, as well as characteristic ultrastructural changes in chromatin.

Key words: C2C12 cells, UVB, Apoptosis, Electron microscopy, TUNEL

Offprint requests to: Prof. Elisabetta Falcieri, Campus Scientifico Sogesta, Località Crocicchia, 61029 Urbino (PU), Italy. e-mail: elisabetta.falcieri@uniurb.it

Introduction

Myotubes are cell syncytia generated, *in vivo* and *in vitro*, by myoblast fusion forming a single multinucleated structure which progressively becomes muscle fibre after a number of morpho-functional changes. While other syncytia, such as the trophoblast, osteoclasts and chondroclasts, generally contain from 3 to about 8 nuclei, muscle fibres can have several hundred to a few thousand nuclei, thus representing very unusual biological models. Many studies have tried to highlight apoptosis in syncytia, shown to possess a certain territorial discontinuity, which is still correlated to the cells initially forming them (Primeau et al., 2002; Al-Nasiry et al., 2006; Yi et al., 2007; Yamaza et al., 2008).

Skeletal muscle apoptosis is not yet a well understood phenomenon, in particular in the case of differentiated cells, where each myonucleus regulates the gene products in a finite fiber volume (Aravamudan et al., 2006) and individual myonuclear apoptosis, as well as complete cell death, can occur (Primeau et al., 2002).

Muscle atrophy, a more diffusely described condition, is characterized by a decrease in muscle mass, protein content, fibre diameter, force production and

fatigue resistance, as well as by changes in fibre type (Ferreira et al., 2008; Schwartz et al., 2008). A progressive structural change in the differentiated phenotype of muscle cells can be observed; it includes disalignment and spatial disorganization of myofibrils with the formation of myofibril-free zones. Initially these changes appear in subsarcolemmal areas around myonuclei, then, in a second phase, they spread throughout the sarcoplasm (Adhihetty et al., 2007).

UVB radiation is a potent apoptosis inducer in many cell types (Hilder et al., 2005; Luchetti et al., 2006; Liu et al., 2007; Pozzi et al., 2007; Paz et al., 2008), apparently in muscle cells as well (Somosy, 2000; Jiang et al., 2005).

It acts by producing oxidative stress through an increase in the generation of Reactive Oxygen Species (ROS), determining signalling events that lead to gene expression changes, lipid peroxidation, DNA damage, and apoptosis (Higuchi, 2004; Rezvani et al., 2006; Afaq et al., 2007; Kanno et al., 2007). Reversible events include temporary structural and functional alterations, while irreversible events are represented by mutations, malignant transformation, the development of abnormal cell forms, and the ultimate consequence of cellular radiation injury which is cell death .

UVB can induce both extrinsic and intrinsic apoptotic pathways and it is still unclear how these pathways are interrelated (Sandri et al., 2001). However, a mitochondrial involvement in UVB-induced apoptosis is certain. In fact, it is well known that UVB irradiation causes an alteration in the mitochondrial outer membrane structure, correlated to a mitochondrial $\Delta\gamma$ loss, causing permeabilization and cytochrome c release (Hilder et al., 2005). Cytochrome c interacts with Apaf-1 (Apoptotic protease activating factor 1), which is a cytosolic protein, to form the apoptosome, a large oligomeric protein complex which causes self-cleavage and activation of caspase-9. In the skeletal muscle cell, activated caspase-9 stimulates the caspase cascade, acting on effector caspases, caspase-3, -6 and-7 (Tews, 2006), which lead the cell to apoptosis (Jackson and O'Farrel, 1993).

Oxidative stress, mitochondrial damage and apoptotic cell death are involved in various muscular disorders, such as Duchenne muscular dystrophy, hereditary inclusion body myopathy, malignant hyperthermia, alcoholic myopathy and mitochondrial myopathies (Sandri et al., 1998; Lee et al; 2005; Tews, 2005; Basset et al., 2006; Abdel et al., 2007; Amsili et al., 2007; Nishida, 2007), however the apoptotic process in skeletal muscle is still only partially understood.

Therefore, the recently described role of apoptosis in a number of muscle pathologies (Ikezoe et al., 2000, 2004; Min-Cheol et al., 2005; Palma et al., 2009) prompted us to investigate this phenomenon, by means of a multiple technical approach in skeletal muscle fibre *in vitro*.

In this work we have analysed C2C12, a muscle murine cell line commonly used as a model for studying skeletal muscle (Burattini et al., 2004). Both myoblasts and myotubes were UVB irradiated and cell response was investigated by means of TEM, SEM, TUNEL, DNA electrophoresis, flow cytometry and caspase Western blotting.

Materials and methods

Cell culture and apoptosis induction

Mouse C2C12 myoblasts were grown in flasks or on coverslips (in dishes), in the presence of Dulbecco's Modified Eagle's Medium (DMEM) supplemented with 10% heat-inactivated Foetal Bovine Serum (FBS), 2mM glutamine at 37° C and 5% CO_2. To induce myogenic differentiation, when 80-100% cell confluence was obtained, the previous medium was substituted with DMEM supplemented with 1% FBS. Cells were analysed at undifferentiated and differentiated stages (7 days after differentiation induction). Differentiation progression was monitored by means of a TE 2000-S Nikon reversed microscope (RM) with a digital Nikon DN100 acquisition system (Zamai et al., 2004; Curci et al., 2008).

To induce apoptosis, myoblasts and myotubes were exposed to 312 nm UVB radiation for 30 minutes at room temperature, at a distance of 1 cm, followed by a 4 hour post-incubation at 37°C in humidified air with 5% CO_2.

To test the effects of caspase inhibitors, C2C12 were incubated with 5 µM caspase-9 and -3 inhibitors (Calbiochem, San Diego, USA) for 2 hours before irradiation and compared to non-irradiated, identically treated C2C12 cells.

Scanning Electron Microscopy (SEM)

Both control and treated myoblasts and myotubes were directly cultured on coverslips in Petri dishes. After careful washing with phosphate buffer, monolayers were fixed with 2.5% glutaraldehyde in 0.1 M phosphate buffer for 1hour, then quickly washed and post-fixed with 1% OsO_4 in the same buffer for 1 hour. After alcohol dehydration, they were critical point dried, gold sputtered and observed with a Philips 515 scanning electron microscope.

Myoblast blebbing was considered a criterion to quantify apoptosis and its behavior in the presence of caspase-9 and -3 inhibitors. The analysis was performed on the whole area (5.29 cm^2) of three different coverslips, and compared to untreated and UVB-treated specimens (Battistelli et al., 2004).

Transmission Electron Microscopy (TEM)

Myoblasts, growing in flasks, were washed and immediately fixed *in situ* with 2.5% glutaraldehyde in 0.1 M phosphate buffer for 15 minutes, then gently scraped and centrifuged at 1200 rpm. Pellets were

additionally fixed for 1hour, alcohol dehydrated, and embedded in araldite. Myotubes, growing on coverslips were identically fixed, but for 1hour and maintaining the monolayer to preserve syncytia morphology as much as possible. They were then post-fixed, dehydrated as described above, and embedded *in situ*. Glass coverslips were removed by dipping specimens in liquid nitrogen and sections were carried out tangentially along the monolayer plane. Thin sectioning was preceded by the analysis of toluidine blue-stained semithin sections which allowed an overall view of the specimen. Thin sections were stained with uranyl acetate and lead citrate and analysed with a Philips CM10 electron microscope (Curci et al., 2008).

TUNEL

Cells, grown on coverslips, were washed and fixed with 4% paraformaldehyde in PBS pH 7.4 for 30 minutes, rinsed with PBS and permeabilized with a mixture 2:1 of ethanol and acetic acid for 5 minutes at -20°C. For the TUNEL technique, all reagents were from Apoptag Plus, D.B.A., Oncor and procedures were carried out according to the manufacturer's instructions. Cells were treated with TdT buffer for 10 minutes at room temperature and incubated with the reaction buffer containing the TdT enzyme for 1 hour at 37°C in a humidified chamber. The reaction was blocked by the stop buffer for 10 minutes. Cells were incubated with a FITC-conjugated anti-digoxigenin antibody for 30 minutes at room temperature. Finally, slides were mounted with an antifading medium. Specimens were observed and photographed with a VANOX (Olympus, Milano, Italy s.r.l.) fluorescence microscope (Smith and Tisdale, 2003).

Gel electrophoresis

$3x10^6$ cells/ml were incubated at 37°C with 20 µl proteinase K and the nucleic acid was extracted following Qiagen kit procedures (Hilden, Germany). 2 µg of DNA per lane were run on 1.8% agarose gel (Bio-Rad, Hercules, CA) in 0.5% Tris, 0.2% borate, 0.2% EDTA 1x buffer, stained with 0.5 µg/ml ethidium bromide and visualized on an UV transilluminator (Bio-Rad Laboratories, Inc., Milano, Italy) (Zamai et al., 2004). Molecular weight marker (MW) was AvaII/EcoRI-pBR322 (low range) (Bio-Rad Laboratories, Inc., Milano, Italy) (Ormerod, 2004).

DNA content evaluation

Undifferentiated and differentiated cells were harvested and fixed with 70% cold (-20°C) ethanol. Samples were washed twice with PBS, then pellets were resuspended in citrate buffer, propidium iodide (PI; 20 µg/ml) and RNAse (100 µg/ml). Samples were kept at 37°C in the dark for at least 30 minutes and analyzed to determine the cell-cycle profile with the use of a FACScalibur flow cytometer equipped with two lasers. Data were acquired and analysed by CellQuest™ flow cytometry software (Becton Dickinson, San Jose, CA).

Assessment of ΔΨm (mitochondrial membrane potential)

To perform MT red CMXRos and JC-1 staining, cells were incubated with dyes for 30 and 10 min at 37°C, respectively, in complete medium. These fluorochromes passively diffuse across the plasma membrane and accumulate in the negatively charged mitochondrial matrix. The extent of dye uptake is dependent upon the size of Δψm; dissipation of Δψm results in a decrease in cell-associated fluorescence that can be detected by flow cytometry.

The mitochondria-specific dye Chloromethyl-X-Rosamine (CMXRos; MitoTracker Red) was used at a concentration of 100 nM to determine Δψm.

JC-1 (5,5',6,6'-tetrachloro-1,1',3,3'-tetraethyl-benzimidazolcarbocyanine iodide) was used at the final concentration of 5 µg/ml (Cossarizza et al., 1993). This dye excites at 488-490 nm, the monomeric form emits at 527 nm, and J-aggregates emit at 590 nm.

In both cases, cells were incubated with fluorochromes in the dark and then assayed by flow cytometry. Suspensions of stained cells were analyzed using a FACScalibur (Becton Dickinson Immunocytometry Systems, San Jose, CA). Forward scatter (FS), side scatter (SS), JC-1 monomers (FL1), JC-1 aggregates (FL2) and CMX-Ros fluorescence (FL3) were collected and analyzed using CellQuest™ software.

Statistical analysis

Flow Cytometric (FC) data (DNA content and mitochondrial membrane potential) were presented as mean ± SE. FC experiments were performed 3 times in duplicate. Significant differences were detected, in regard to CMXRos data, between control myoblasts and UVB irradiated myoblasts, as in control myotubes and UVB irradiated ones.

For DNA content evaluation and cell cycle phase discrimination, data were *quasi* significant.

Statistical significance was determined using a paired Student's *t*-test. Data were presented as means ± SE. Mean values were considered significantly different at $P<0.05$.

Protein assay

This was performed using the Bio-Rad Protein Assay according to the manufacturer's instructions.

Preparation of cell homogenates and caspase Western blot analysis

Cells were washed twice in phosphate-buffered saline (PBS, pH 7.4) containing the Complete Protease Inhibitor Cocktail supplemented with 1 mM Na3VO4.

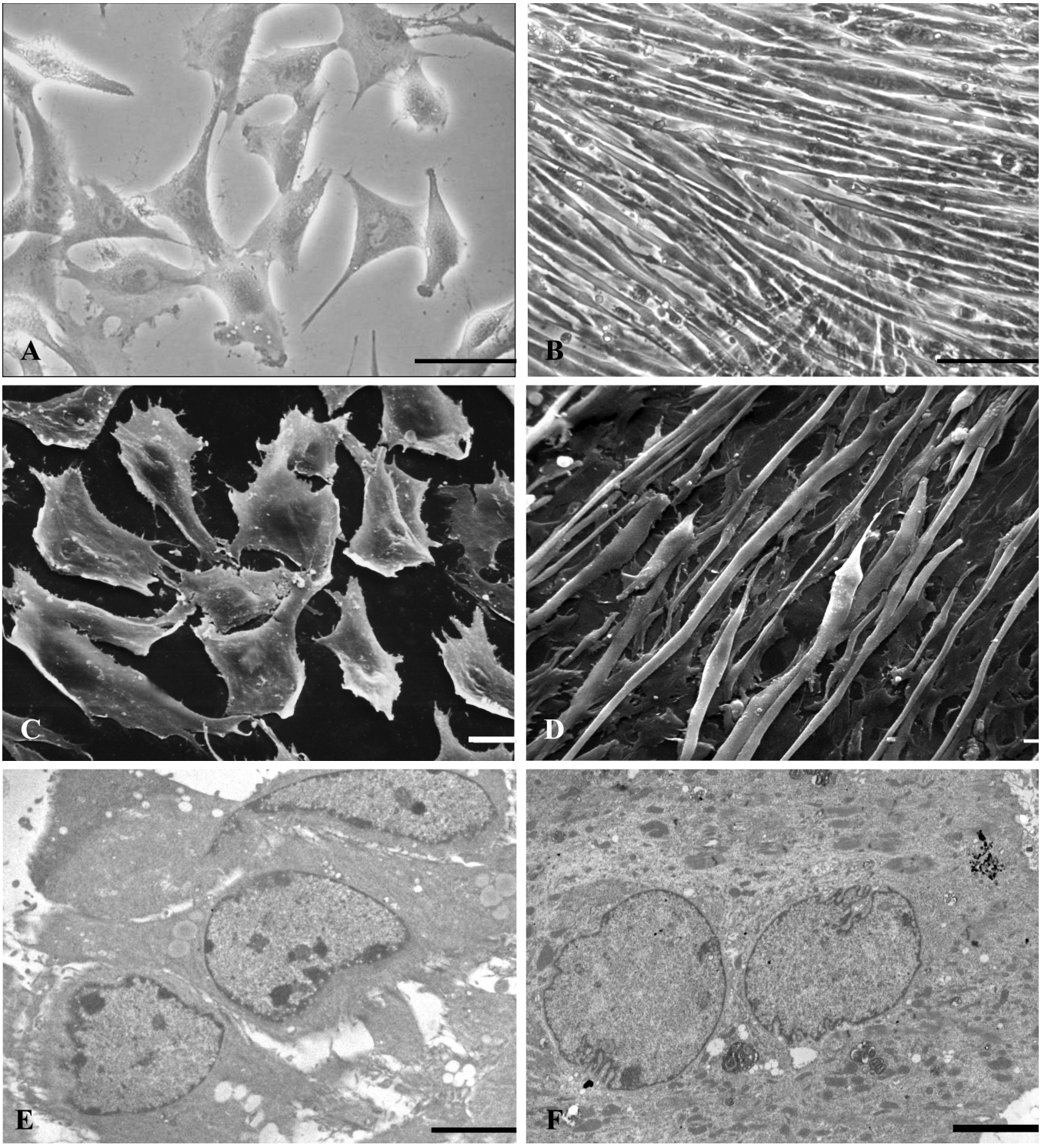

Fig. 1. Control myoblasts **(A, C, E)** and myotubes **(B, D, F)**, analysed at RM **(A, B)**, SEM **(C, D)** and TEM **(E, F)**. Cell surface appears smooth, with occasional microvilli, in both conditions **(C, D)**. Inner cell ultrastructural analyses **(E, F)** evidences a good preservation of organellar components, in particular the large number of mitochondria present in myotubes **(F)**. Scale bars: A, C, D, 10 µm; B, 20 µm; E, 1 µm; F, 2 µm

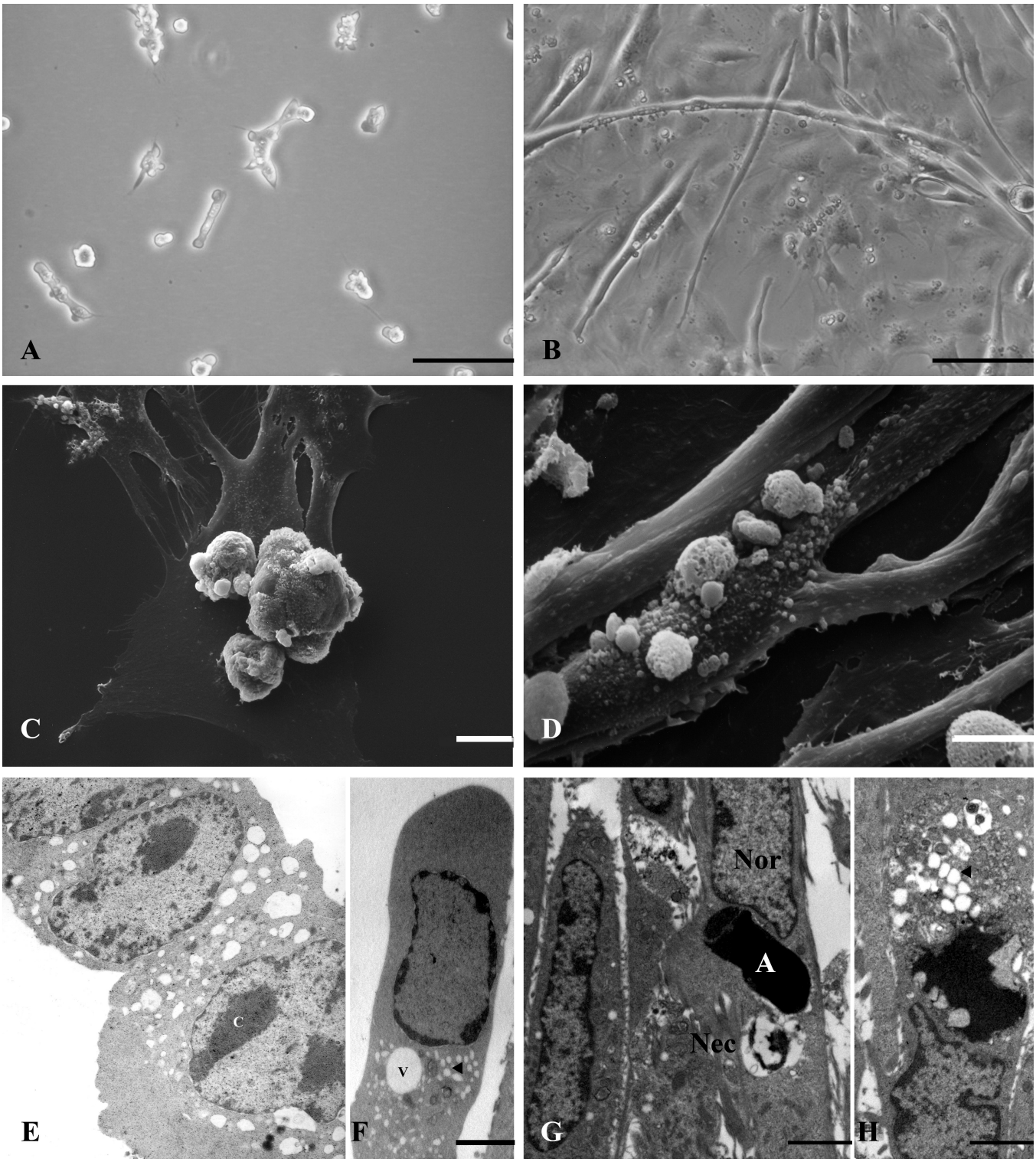

Fig. 2. Both myoblasts **(A, C, E, F)** and myotubes **(B, D, G, H)**, at RM **(A, B)**, SEM **(C, D)** and TEM **(E, F, G, H)** evidence profound changes after UVB-treatment. Monolayer organization appears greatly modified when compared to controls and cell surface undergoes a diffuse blebbing **(C, D)**. A general vacuolization **(E, F, H)** (v) and mitochondrial swelling **(F, H)** (triangle) appear. Myoblast nuclei show apoptotic changes at TEM **(F)** and the presence of non- apoptotic (Nor), apoptotic (A) and necrotic (Nec) nuclei can be occasionally revealed in the same myotube **(G)**. Scale bars: A, 20 μm; B, C, D, 10 μm; E, F, 1 μm; G, H, 2 μm

Cells were lysed at 10^7/ml in boiling electrophoresis sample buffer containing the protease inhibitor cocktail. Lysates were then briefly sonicated to shear DNA and reduce viscosity, and boiled for 5 minutes to solubilize protein. Protein separated on sodium dodecylsulphate polyacrylamide gel electrophoresis (SDS-PAGE) was transferred to nitrocellulose membranes using a semidry blotting apparatus. Membranes were saturated for 60 minutes at 37°C in blocking buffer (PBS supplemented with 5% non-fat milk), then incubated overnight at 4°C in blocking buffer containing the primary antibody. After four washes in PBS containing 0.1% Tween 20, samples were incubated for 30 minutes at room temperature with peroxidase-conjugated secondary antibody diluted 1:5000 in PBS-Tween 20, and washed as above. Bands were visualized by the ECL method. The statistical analysis of Western blotting data was performed by densitometric scanning (Falà et al., 2008).

Results

Control myoblasts observed at RM appeared separated by wide intercellular spaces, either star-shaped or fusiform, with one large central nucleus (Fig. 1A). Long multi-nucleated myotubes, in close contact with each other (Fig. 1B), were present in the differentiated condition.

Cell surface analysis, performed with SEM, showed a relatively smooth cell surface, with occasional microvilli both at undifferentiated and differentiated stage (Fig. 1C,D). TEM revealed good organelle preservation (Fig. 1E,F) and clearly recognizable nuclear domains. In particular, a large number of mitochondria appeared in myotubes (Fig. 1F). UVB irradiated samples

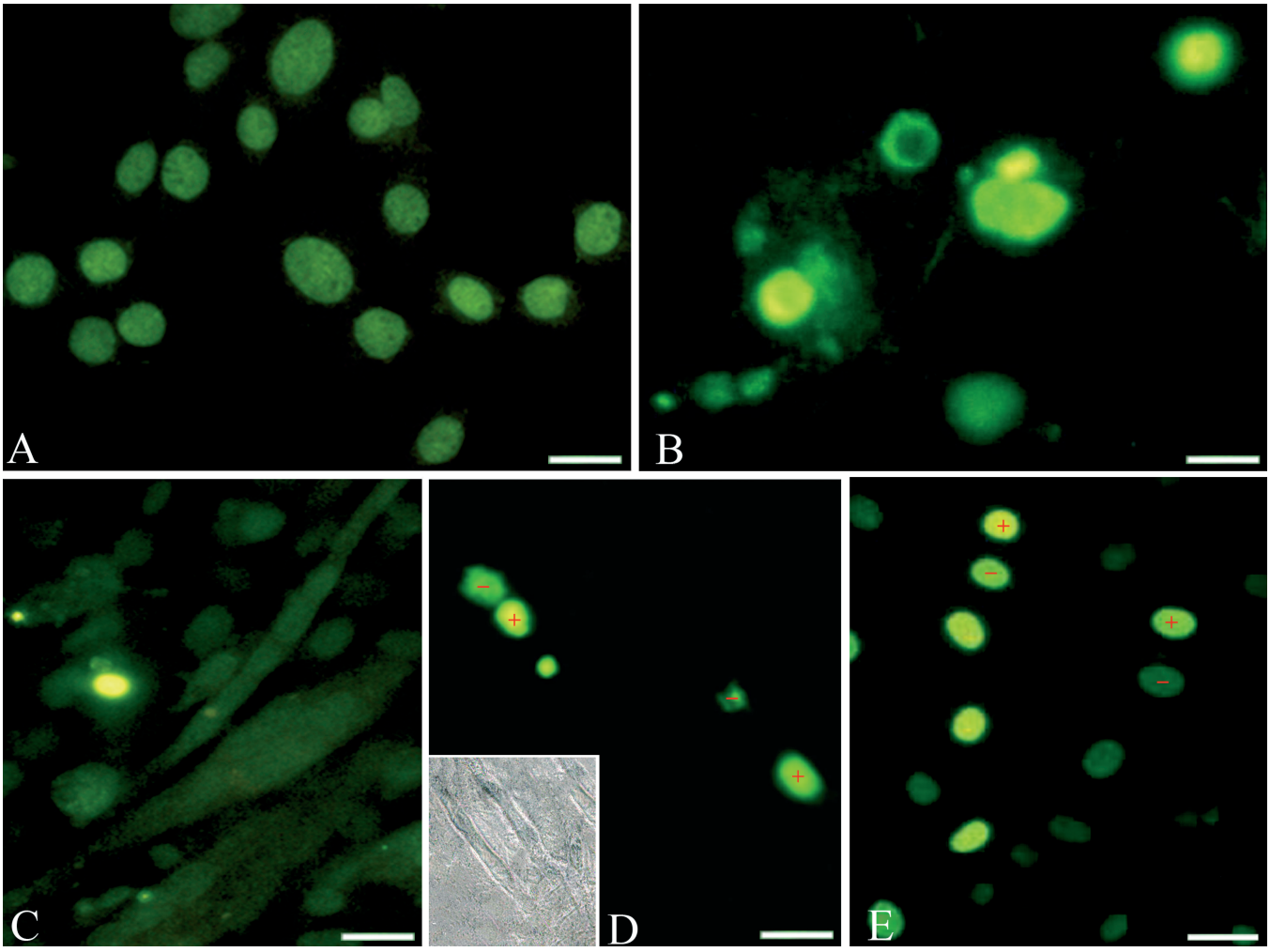

Fig. 3. C2C12 undifferentiated **(A)** and differentiated **(C)** control cells appear TUNEL negative. Differently, both UVB-irradiated myoblasts **(B)** and myotubes **(D, E)** result TUNEL positive. Myotubes, better observable also in phase contrast (**D**, inset), are characterized by the presence of positive (+) and negative (-) nuclei in the same cell **(D, E)**. Nuclear fluorescence appears diffuse. Scale bars: 30 µm.

revealed profound changes in monolayer organization, as well as significant surface and inner-cell ultrastructural alterations. Large cell-free spaces appeared in the myoblast monolayer and cells showed progressive bleb formation (Fig. 2A,C). A characteristic increase in the anchorage to the underlying substrate, revealed by the resistance to trypsin treatment (at least 20 minutes *vs* 5 minutes for control condition) also appeared (not shown). In differentiated conditions, UVB caused a massive myotube detachment from the substrate (Fig. 2B), and again, bleb formation clearly evidenced by SEM (Fig. 2D).

TEM of UVB-irradiated myoblasts revealed a general cytoplasmic vacuolization (Fig. 2E,F) and frequently, a characteristic chromatin margination at the nuclear periphery, sharply separated from the diffuse form. Even if dense, cup-shaped masses, comparable to those of more classic apoptotic models (Falcieri et al., 1994; Shiokawa et al., 2002) could not be found, the evidenced nuclear features, when analysed in detail, appear to suggest apoptosis. Cell vacuolization could also be revealed in UVB-treated myotubes, as well as apoptotic patterns. Interestingly, apoptotic, non apoptotic and necrotic nuclei could occasionally be observed within the same myotube (Fig. 2G,H).

After UVB radiation both cell conditions showed a certain positivity to the TUNEL reaction (Fig. 3), even if in an unusual manner: in fact, cup-shaped apoptotic chromatin and micronuclei were rarely detected, but the common pattern of apoptotic nuclei was represented by a diffuse fluorescence (Fig. 3B,D,E). TUNEL also revealed the presence of positive and negative nuclei in the same myotube, as could be better observed by coupling fluorescence and phase contrast microscopy (Fig. 3D). This discontinuous fluorescence distribution within the same myotube can be correlated, in our opinion, with TEM observations, contemporarily revealing both living and dead nuclei. All this suggests unusual DNA behavior and is supported by gel electrophoresis assays that did not show oligo-nucleosomal DNA fragmentation in irradiated myoblasts nor in myotubes (Fig. 4).

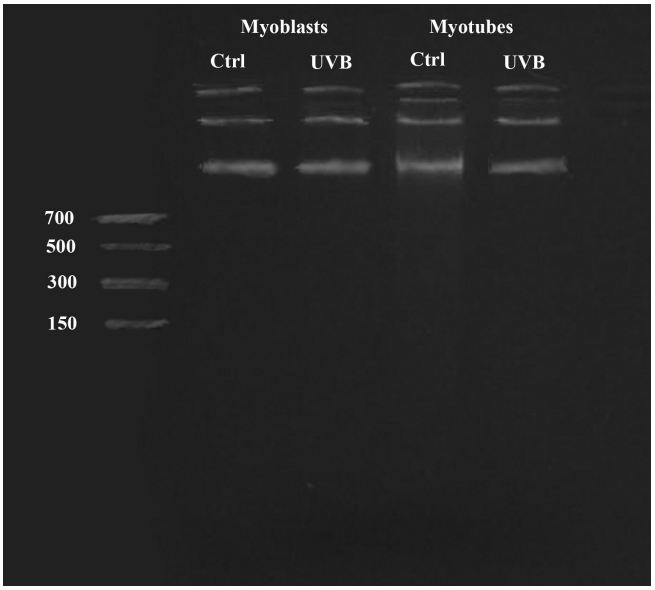

Fig. 4 Agarose gel electrophoresis. Oligonucleosomal DNA fragmentation is absent both in irradiated myoblasts and myotubes.

This behavior is mostly in agreement with cell cycle analysis performed by flow cytometry, where an evident hypodiploid peak could not be revealed.

Cell-cycle phase investigation showed a certain stability in myotubes in both control and UVB irradiated samples.

Differently, irradiated myoblasts showed a slightly higher percentage of S and G2/M events (20±3% and 22±2%, respectively) in comparison to control myoblasts (14±2% and 15±1.5%, respectively, $p \leq 0.5$) (Fig. 5). This could be due to a possible radiation-induced G2/M block, frequently observed in cells which are still dividing. In myotubes, which have lost the ability to re-enter the cell cycle, S and G2/M phase events were comparable in control and treated specimens.

Flow cytometry was used to investigate, in both conditions, mitochondrial membrane potential response to UVB-radiation. MT red CMXRos and JC-1 (data not shown) analyses were conducted (Fig. 6, 7) in both control and UVB conditions. In UVB irradiated cells, histograms showed a decrease in mitochondrion-specific probe fluorescence (Fig. 6, 7). Furthermore, it was possible to observe a different type of fluorescence loss in myoblasts with respect to myotubes (Fig. 6): in fact, in the latter a bimodal distribution seems to represent a possible coexistence of collapsed and functional mitochondria.

Mitochondrial involvement can be further confirmed by the study of caspase behavior, analysed by Western blot. In irradiated samples, caspase-9 and -3 cleavage (Fig. 8A,B) could be observed, while caspase-8 cleavage (typical of the extrinsic pathway) was not revealed (Fig. 8C).

The utilization of caspase-9 and -3 inhibitors seemed to markedly, if not completely, reduce apoptosis. In particular, SEM analysis showed 30% myoblasts with surface blebbing. The percentage considerably decreased to 17% and 13% using caspase-9 and -3 inhibitors, respectively (Fig. 9). The same study was not possible on myotubes because the monolayer architecture did not permit a reliable cell count.

Discussion

All the results obtained from our studies indicate that, even if skeletal muscle cells have been long considered relatively resistant to apoptosis, UVB irradiation apparently induces it in C2C12 cells, where it has been proven by a several pieces of morphological

and biochemical evidence. RM, SEM and TEM show apoptotic cell features, but they are only partially comparable to those widely described in classical apoptotic models: in fact, cup-shaped dense chromatin, nuclear pore clustering and micronuclei can never, or very rarely, be identified, while early chromatin margination and occasional micronuclei seem to be the most common ultrastructural markers (Stuppia et al., 1996). This behavior can be correlated to the appearance after the TUNEL reaction, which mainly shows a diffuse fluorescence rather than fluorescent cup-shaped patches. TUNEL patterns presumably reflect the lack of oligonucleosomal DNA cleavage, indicated by gel electrophoresis and flow cytometry cell cycle analysis: the presence of a ladder and/or an easily recognizable subdiploid peak can never be revealed (Grzanka et al., 2006). This behavior of C2C12 cells could depend on the apoptotic trigger: in fact, DNA cleavage was reported by Smith and Tisdale, 2003, after treatment with a tumour-derived proteolysis-inducing factor. Furthermore, flow cytometry seems to indicate a certain G2/M arrest in UVB irradiated myoblasts, showing a 22% G2/M event percentage, *vs* 15% in the controls. Differently, treated myotubes appear comparable to

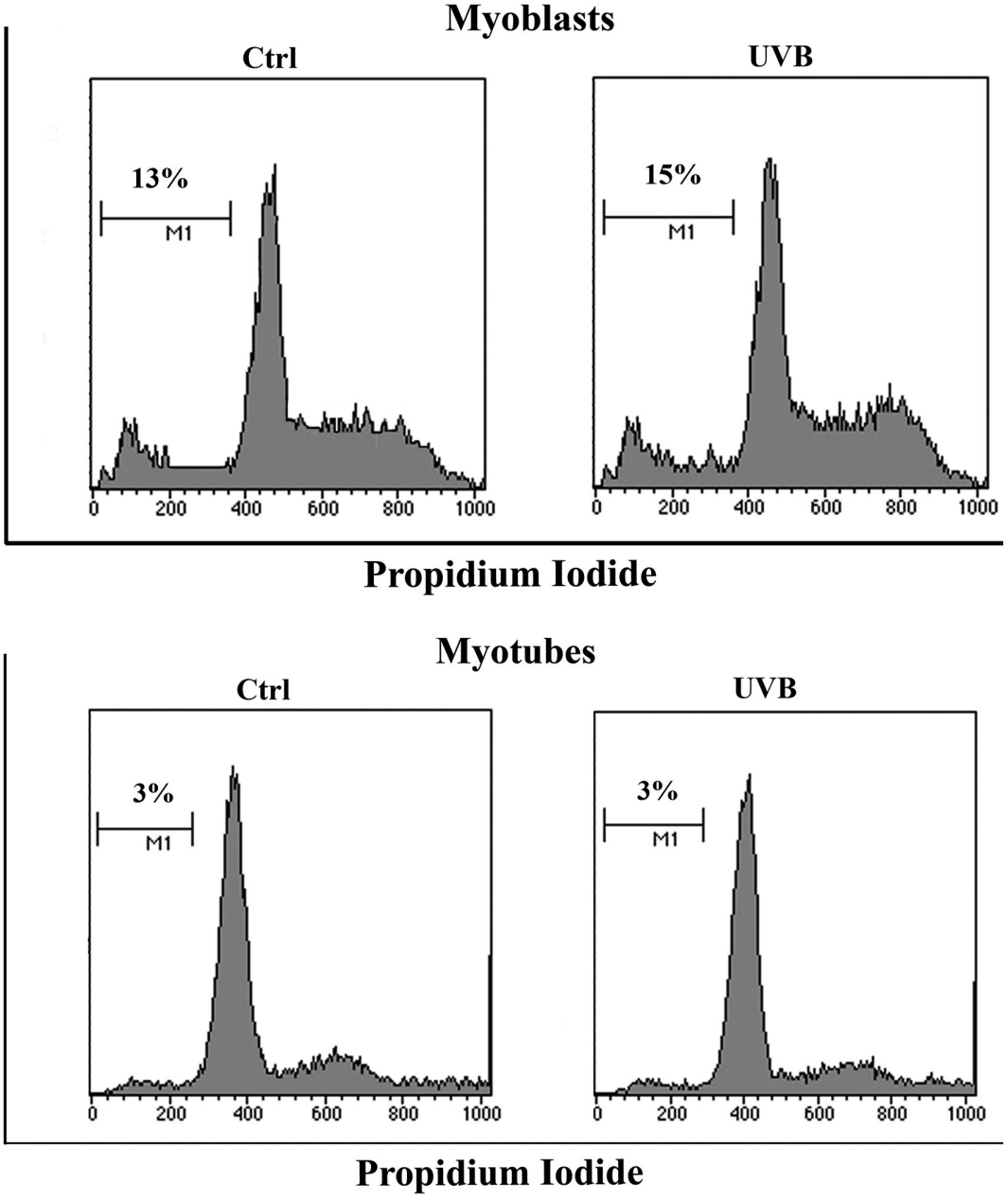

Fig. 5. DNA content evaluation of C2C12 myoblasts and myotubes, respectively. It is possible to observe the lack of subdiploid peak, particularly in UVB irradiated myotubes.

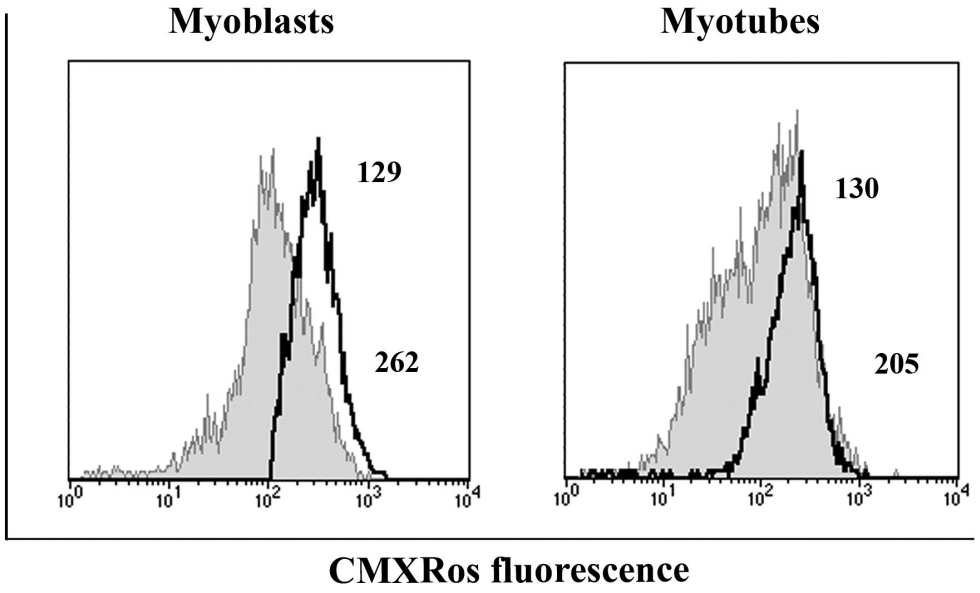

Fig. 6. Mitochondrial membrane potential evaluation in control (empty histogram) and UVB irradiated (filled histogram) in myoblasts and myotubes, by means of CMXRos labelling. Histograms show the decrease in mitochondrial membrane potential occurring in cells after UVB irradiation. Furthermore, it is possible to observe a different type of fluorescence loss in myoblasts when compared to myotubes: in fact in the latter a bimodal distribution seems to represent a possible coexistence of collapsed and functional mitochondria.

untreated ones. Therefore C2C12 seem to be a relatively resistant cell line, in particular when these cells differentiate into myotubes.

An intriguing behavior is an increase in myoblast substrate anchorage, which is expressed through a prolonged (up to 20 min) trypsin resistance. This could be interpreted as an effect of UVB treatment on the cytoskeleton (Luchetti et al., 2004), although independent of apoptotic response. Further studies are in progress to better highlight this phenomenon.

The behavior of mitochondria was then analysed.

TEM observations reveal that mitochondria, as in other experimental models such as hemopoietic ones (Luchetti et al., 2006), are deeply affected by UVB-treatment. Moreover, there is a decrease in mitochondrial membrane potential, as highlighted in flow cytometry, by MT red CMXRos. In particular, such probes show a different fluorescence pattern in myotubes *vs* myoblasts as described. In fact, in myotubes it is possible to observe the coexistence of collapsed and functional mitochondria, presumably correlated to a larger number of mitochondria in the myotube.

Finally, Western blot analysis of caspase activity shows caspase-9 and -3 cleavage, while no activation can be demonstrated for caspase-8. Moreover, the response to caspase-9 and -3 inhibitors, which seem to partially prevent apoptosis, indirectly suggests the presence of intrinsic pathway activation. In particular, there is no relevant difference between the inhibition of caspase-9, which acts only on the intrinsic apoptotic pathway, and that of caspase-3, involved both in the intrinsic and extrinsic pathway (17% *vs* 12% of cell blebbing presence). This result suggests a massive activation of the apoptotic mitochondrial pathway, as also indicated indirectly by flow cytometry analyses of

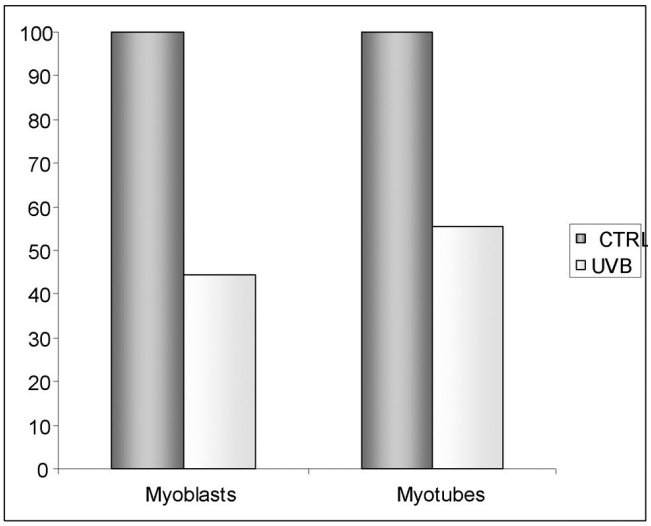

Fig. 7. Histograms showing changes in mitochondrial membrane potential ($\Delta\Psi m$) after UVB irradiation (in a representative experiment). Mitochondrial alterations are significant ($p<0,05$) in both conditions, although a more pronounced reduction in myoblasts $\Delta\Psi m$ vs myotubes is evident.

mitochondrial functionality, which does not exclude, in any case, an extrinsic apoptotic pathway.

We can conclude that UVB irradiation, causing an overproduction of ROS (Kovacs et al., 2009), triggers apoptosis in skeletal muscle cells in both undifferentiated and differentiated conditions. Cell death is partially due to mitochondrial damage followed by cytochrome c release that determines the activation of caspase-9 and, subsequently, the caspase cascade leading

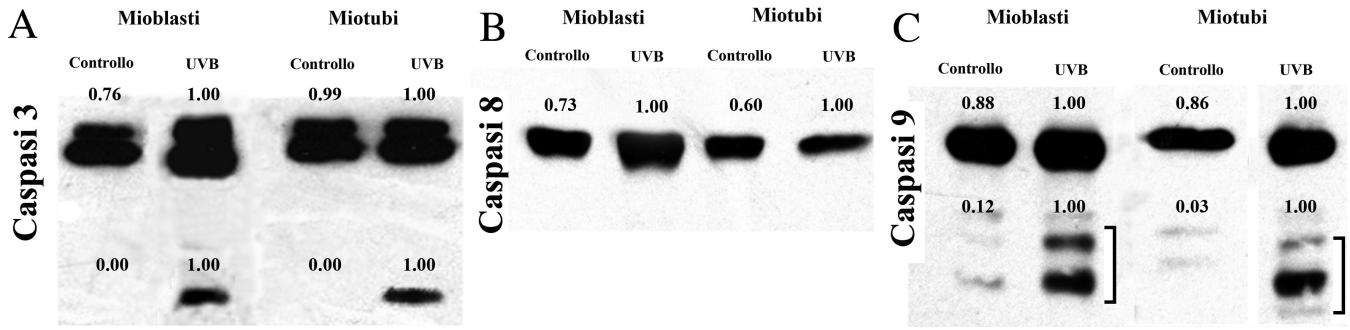

Fig. 8. Western blot analyses. In irradiated samples a caspase-9 and -3 cleavage **(A, B)** is clear, while that of caspase-8 is not revealed **(C)**. For the blots, protein levels were quantified by using Image J software as described under Materials and Methods. Band intensities of UVB treated specimens were normalized to 1, and control samples were expressed as fraction.

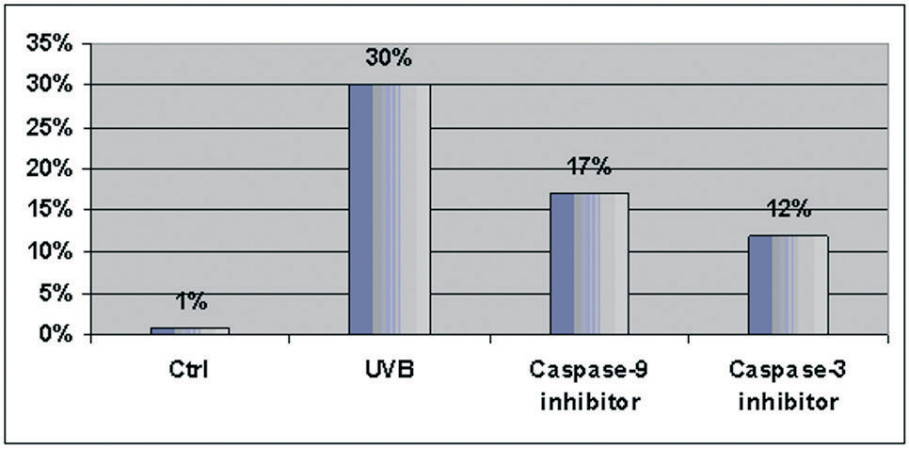

Fig. 9. Histogram of cell blebbing percentages from SEM analyses on 3 coverslips per condition (in a representative experiment): a 30% myoblast blebbing of UVB-treated specimens is reduced to 17% and 13% using caspase-9 and -3 inhibitors, respectively.

to cell apoptosis.

Nevertheless, C2C12 cells seem to be less responsive to apoptosis, especially at the differentiated stage, if compared to hemopoietic cells. In particular, their apoptotic morphological and biochemical features, when present, are different from those of most cell lines.

In myotubes, a very unusual cell model as are all syncytia, we have noticed the presence of apoptotic, non-apoptotic and necrotic nuclei in the same fiber. A possible interpretation of this phenomenon is that the myotube, deriving from the fusion of a number of mononucleated cells, presumably maintains a certain morpho-functional territorial organization (Primeau et al., 2002; Al-Nasiry et al., 2006; Yi et al., 2007; Bruusgaard and Gundersen, 2008; Yamaza et al., 2008), which determines independent apoptotic responses in the various nuclei. In a previous work, concerning the syncytiotrophoblast, a very different model which undergoes apoptosis in particular conditions, we have already discussed this feature (Battistelli et al., 2004) .

The aim of this work was to investigate the apoptotic behavior of the C2C12 cell line with the purpose of highlighting cell death in skeletal muscle tissue which has been long considered very resistant. Programmed muscle cell death has been reported (Schwartz, 2008) after denervation and also during development, in tendon-muscle crosstalk failure (Rodriguez-Guzman et al., 2007). Moreover, it is well known (Amsili et al., 2007; Nishida et al., 2007) that apoptosis is involved in some types of neuromuscular disorders, such as Duchenne Muscular Dystrophy and some other muscle diseases which are characterized by an involvement of oxidative stress and a loss of muscle fibres.

The study of apoptosis in the skeletal muscle cell appears to be extremely important in identifying cell markers as potential prognostic and therapeutic targets.

Our work suggests that apoptosis occurs in the absence of nucleosomic DNA cleavage, but in the presence of a certain diffuse double-strand DNA fragmentation. Typical apoptotic chromatin changes also appear, together with the presence of non-apoptotic, apoptotic and necrotic nuclei in the myotube, within the same syncytium.

Aknowledgements: Dr. C. Squillace, Dr. D. Curzi, Mr. A. Valmori and Mr. O. Rusciadelli are thanked for skilful technical assistance.

References

Abdel S.E., Abdel-Meguid I. and Korraa S. (2007). Markers of oxidative stress and aging in Duchene muscular dystrophy patients and the possible ameliorating effect of He:Ne laser. Acta Myol. 26,14-21.

Adhihetty P.J., O'Leary M.F., Chabi B., Wicks K.L. and Hood D.A. (2007). Effect of denervation on mitochondrially mediated apoptosis in skeletal muscle. J. Appl. Physiol. 102,1143-1451.

Afaq F., Syed D.N., Malik A., Hadi N., Sarfaraz S., Kweon M.H., Khan N., Zaid M.A. and Mukhtar H. (2007). Delphinidin, an anthocyanidin in pigmented fruits and vegetables, protects human HaCaT keratinocytes and mouse skin against UVB-mediated oxidative stress and apoptosis. J. Invest. Dermatol. 127, 222-232.

Al-Nasiry S., Spitz B., Hanssens M., Luyten C. and Pijnenborg R. (2006). Differential effects of inducers of syncytialization and apoptosis on BeWo and JEG-3 choriocarcinoma cells. Hum. Reprod. 21,193-201.

Amsili S., Shlomai Z., Levitzki R., Krause S., Lochmuller H., Ben-Bassat H. and Mitrani-Rosenbaum S. (2007). Characterization of hereditary inclusion body myopathy myoblasts: possible primary impairment of apoptotic events. Cell Death Differ. 14,1916-1924.

Aravamudan B., Mantilla C.B., Zhan W.Z. and Sieck G.C. (2006). Denervation effects on myonuclear domain size of rat diaphragm fibers. J. Appl. Physiol. 100, 1617-1222.

Basset O., Boittin F.X., Cognard C., Constantin B. and Ruegg U.T. (2006). Bcl-2 overexpression prevents calcium overload and subsequent apoptosis in dystrophic myotubes. Biochem. J. 395, 267-76.

Battistelli M., Burattini S., Pomini F., Scavo M., Caruso A. and Falcieri E. (2004). Ultrastructural study on human placenta from intrauterine growth retardation cases. Microsc. Res. Tech. 65, 150-158.

Bruusgaard J.C. and Gundersen K. (2008). In vivo time-lapse microscopy reveals no loss of murine myonuclei during weeks of muscle atrophy. J Clin Invest. 118, 450-457.

Burattini S., Ferri P., Battistelli M., Curci R., Luchetti F. and Falcieri E. (2004). C2C12 murine myoblasts as a model of skeletal muscle development: morpho-functional characterization. Eur. J. Histochem. 48, 223-233.

Cossarizza A., Baccarani-Contri M., Kalashnikova G. and Franceschi C. (1993). A new method for the cytofluorimetric analysis of mitochondrial membrane potential using the J-aggregate forming lipophilic cation 5,5',6,6'-tetrachloro-1,1',3,3' tetraethylbenzimidazolcarbocyanine iodide (JC-1). Biochem. Biophys. Res. Commun. 197, 40-45.

Curci R., Battistelli M., Burattini S., D'Emilio A., Ferri P., Lattanzi D., Ciuffoli S., Ambrogini P., Cuppini R. and Falcieri E. (2008). Surface and inner cell behaviour along skeletal muscle cell in vitro differentiation. Micron 39, 843-851.

Falà F., Blalock V.L., Tazzari P.L., Cappellini A., Chiarini F., Martinelli G., Tafuri A., McCubrey J.A., Cocco L. and Martelli A.M. (2008). Proapoptotic activity and chemosensitizing effect of the novel Akt inhibitor (2S)-1-(1H-Indol-3-yl)-3-[5-(3-methyl-2H-indazol-5-yl)pyridin-3-yl]oxypropan2-amine (A443654) in T-cell acute lymphoblastic leukemia. Mol. Pharmacol. 74, 884-895.

Falcieri E., Gobbi P., Zamai L. and Vitale M. (1994). Ultrastructural features of apoptosis. Scanning Microsc. 8, 653-65.

Ferreira R., Neuparth M.J., Vitorino R., Appell H.J., Amado F. and Duarte J.A. (2008). Evidences of apoptosis during the early phases of soleus muscle atrophy in hindlimb suspended mice. Physiol. Res. 57, 601-611.

Grzanka D., Domaniewski J., Grzanka A. and Zuryn A. (2006). Ultraviolet radiation (UV) induces reorganization of actin cytoskeleton in CHOAA8 cells. Neoplasma 53, 328-332.

Higuchi Y. (2004). Glutathione depletion-induced chromosomal DNA fragmentation associated with apoptosis and necrosis. J. Cell Mol. Med., 8, 455-464.

Hilder T.L., Carlson G.M., Haystead T.A., Krebs E.G. and Graves L.M. (2005). Caspase-3 dependent cleavage and activation of skeletal muscle phosphorylase b kinase. Mol. Cell Biochem. 275, 233-242.

Ikezoe K., Yan C., Momoi T., Imoto C., Minami N., Ariga M., Nihei K. and Nonaka I. (2000). A novel congenital myopathy with apoptotic changes. Ann. Neurol. 47, 531-536.

Ikezoe K., Nakagawa M., Osoegawa M., Kira J. and Nonaka I. (2004). Ultrastructural detection of DNA fragmentation in myonuclei of fatal reducing body myopathy. Acta Neuropathol. 107, 439-442.

Jackson M.J. and O'Farrell S. (1993). Free radicals and muscle damage. Br. Med. Bull., 49, 630-641.

Jiang B., Xiao W., Shi Y., Liu M. and Xiao X. (2005). Heat shock pretreatment inhibited the release of Smac/DIABLO from mitochondria and apoptosis induced by hydrogen peroxide in cardiomyocytes and C2C12 myogenic cells. Cell Stress Chaperones 10, 252-62.

Kanno S., Kakuta M., Kitajima Y., Osanai Y., Kurauchi K., Ohtake T., Ujibe M., Uwai K., Takeshita M. and Ishikawa M. (2007). Preventive effect of trimidox on oxidative stress in U937 cell line. Biol. Pharm. Bull. 30, 994-998.

Kovacs D., Raffa S., Flori E., Aspite N., Briganti S., Cardinali G., Torrisi M.R. and Picardo M. **(**2009). Keratinocyte growth factor down-regulates intracellular ROS production induced by UVB. J. Dermatol. Sci. 54, 106-113.

Lee M.H., Jang M.H., Kim E.K., Han S.W., Cho S.Y. and Kim C.J. (2005). Nitric oxide induces apoptosis in mouse C2C12 myoblast cells. J. Pharmacol. Sci. 97, 369-376.

Liu S., Mizu H. and Yamauchi H. (2007). Molecular response to phototoxic stress of UVB-irradiated ketoprofen through arresting cell cycle in G2/M phase and inducing apoptosis. Biochem. Biophys. Res. Commun. 364, 650-655.

Luchetti F., Canonico B., Mannello F., Masoni C., D'Emilio A., Battistelli M., Papa S. and Falcieri E. (2007). Melatonin reduces early changes in intramitochondrial cardiolipin during apoptosis in U937 cell line. Toxicol. In Vitro 21, 293-301.

Luchetti F., Canonico B., Curci R., Battistelli M., Mannello F, Papa S., Tarzia G. and Falcieri E. (2006). Melatonin prevents apoptosis induced by UV-B treatment in U937 cell line. J. Pineal Res. 40, 158-167.

Luchetti F., Mannello F., Canonico B., Battistelli M., Burattini S., Falcieri E. and Papa S. (2004). Integrin and cytoskeleton behaviour in human neuroblastoma cells during hyperthermia-related apoptosis. Apoptosis 9, 635-648.

Min-Cheol L., Gye-Ryoung W. and Jae-Hyoo K**. (**2005). Apoptosis of Skeletal Muscle on Steroid-Induced Myopathy in Rats. J. Nutr. 135, 1806S-1808S.

Nishida H., Ichikawa H. and Konishi T. (2007). Shengmai-san enhances antioxidant potential in C2C12 myoblasts through the induction of intracellular glutathione peroxidase. J. Pharmacol. Sci. 105, 342-352.

Ormerod M.G. (2004). Cell-cycle analysis of asynchronous populations. Methods Mol. Biol. 263, 345-354.

Palma E., Tiepolo T., Angelin A., Sabatelli P., Maraldi N.M., Basso E., Forte M.A., Bernardi P. and Bonaldo P. (2009). Genetic ablation of cyclophilin D rescues mitochondrial defects and prevents muscle apoptosis in collagen VI myopathic mice. Hum. Mol. Genet. Mar. 17.

Paz M.L., González Maglio D.H., Weill F.S., Bustamante J. and Leoni J. (2008). Mitochondrial dysfunction and cellular stress progression after ultraviolet B irradiation in human keratinocytes. Photodermatol. Photoimmunol. Photomed. 24, 115-122.

Pozzi D., Grimaldi P., Gaudenzi S., Di Giambattista L., Silvestri I., Morrone S. and Congiu Castellano A. (2007). UVB-radiation-induced apoptosis in Jurkat cells: a coordinated fourier transform infrared spectroscopy-flow cytometry study. Radiat. Res. 168, 698-705.

Primeau A.J., Adhihetty P.J. and Hood D.A. (2002). Apoptosis in heart and skeletal muscle. Can. J. Appl. Physiol. 27, 349-395.

Rezvani H.R., Mazurier F., Cario-André M., Pain C., Ged C., Taïeb A. and de Verneuil H. (2006). Protective effects of catalase overexpression on UVB-induced apoptosis in normal human keratinocytes. J. Biol. Chem. 281, 17999-18007.

Rodriguez-Guzman M., Montero J.A., Santesteban E., Gañan Y., Macias D. and Hurle J.M. (2007). Tendon-muscle crosstalk controls muscle bellies morphogenesis, which is mediated by cell death and retinoic acid signalling. Dev. Biol. 302, 267-80.

Sandri M., Minetti C., Pedemonte M. and Carraro U. (1998). Apoptotic myonuclei in human Duchenne muscular dystrophy. Lab. Invest. 78, 1005-1016.

Sandri M., El Meslemani A.H., Sandri C., Schjerling P., Vissing K., Andersen J.L., Rossini K., Carraro U. and Angelini C. (2001). Caspase 3 expression correlates with skeletal muscle apoptosis in Duchenne and facioscapulo human muscular dystrophy. A potential target for pharmacological treatment? J. Neuropathol. Exp. Neurol. 60, 302-312.

Schwartz LM. (2008). Atrophy and programmed cell death of skeletal muscle. Cell Death Differ. 15, 1163-1169.

Shiokawa D., Kobayashi T. and Tanuma S. (2002). Involvement of DNase gamma in apoptosis associated with myogenic differentiation of C2C12 cells. J. Biol. Chem. 277, 31031-31037.

Smith H.J. and Tisdale M.J. (2003). Induction of apoptosis by a cachectic-factor in murine myotubes and inhibition by eicosapentaenoic acid. Apoptosis 8, 161-169.

Somosy Z. (2000). Radiation response of cell organelles. Micron 31, 165-181.

Stuppia L., Gobbi P., Zamai L., Palka G, Vitale M. and Falcieri E. (1996). Morphometric and functional study of apoptotic cell chromatin. Cell Death Differ. 3, 397-405.

Tews D.S. (2005). Muscle-fiber apoptosis in neuromuscular diseases. Muscle Nerve 32, 443-458.

Tews D.S. (2006). Characterization of initiator and effector caspase expressions in dystrophinopathies. Neuropathology 26, 24-31.

Yamaza T., Miura Y., Bi Y., Liu Y., Akiyama K., Sonoyama W., Patel V., Gutkind S., Young M., Gronthos S., Le A., Wang C.Y., Chen W. and Shi S. (2008). Pharmacologic stem cell based intervention as a new approach to osteoporosis treatment in rodents. PLoS ONE 3, e2615.

Yi T., Baek J.H., Kim H.J., Choi M.H., Seo S.B., Ryoo H.M., Kim G.S. and Woo K.M. (2007). Trichostatin A-mediated upregulation of p21(WAF1) contributes to osteoclast apoptosis. Exp. Mol. Med. 39, 213-221.

Zamai L., Burattini S., Luchetti F., Canonico B., Ferri P., Melloni E., Gonelli A., Guidotti L., Papa S. and Falcieri E. (2004). In vitro apoptotic cell death during erythroid differentiation. Apoptosis 9, 235-246.

Accepted July 10, 2009